Journal of MATERIALS RESEARCH

Article
DOI:10.1557/s43578-024-01368-8

Energy harvesting with thermoplastic polyurethane nanofiber mat integrated with functionalized multiwalled carbon nanotubes

Julia I. Salas[1], Sk Shamim Hasan Abir[1], Diego de Leon[1], Ignacio Serrato III[1], Horacio Vasquez[1], Karen Lozano[1,a)], M. Jasim Uddin[1,2,a)]

[1] Department of Mechanical Engineering, University of Texas Rio Grande Valley, Edinburg, TX 78539, USA
[2] Department of Physics and Astronomy, University of Texas Rio Grande Valley, Edinburg, TX 78539, USA
[a)] Address all correspondence to these authors. e-mails: karen.lozano@utrgv.edu; mohammed.uddin@utrgv.edu

Received: 16 November 2023; accepted: 29 May 2024; published online: 17 June 2024

Triboelectric nanogenerators (TENGs) have received considerable attention as flexible and stretchable systems capable of harvesting energy and converting mechanical into electrical energy. This paper reports on Forcespinning-synthesized poly(vinylidene fluoride) (PVDF) and thermoplastic polyurethane (TPU) nanofiber (NF) membranes based TENG. To improve the TENG, the TPU NFs were decorated with multi-walled carbon nanotubes (MWCNT) functionalized with fluoride, amide, and carboxylic groups. The NF demonstrated a stronger interaction with the carboxylic-functionalized MWCNT (c-MWCNT). Furthermore, the c-MWCNT functionalized TPU/PVDF TENGs were evaluated by applying compressive force (30 psi) utilizing a pneumatic cylinder. The maximum alternating voltage, and current outputs were 158 V and 170 μA respectively. The TENG charging capacity for the samples dipped for 12 h in the c-MWCNT showed an ability to charge a 1 μF capacitor up to 3.03 V in 25 s of hand tapping, suggesting that the fabricated TENG has the capability to function as a self-charging flexible energy harvester.

Introduction

In recent years, the world has seen significant usage of portable electronic devices, these have become an integral part of daily life, not only as communication systems but also in the use of sensors and actuators that monitor and assist technical operations in the transportation, manufacturing, and biomedical fields, to mention just a few [1–4]. These devices need an external power source, usually a battery. Powering micro/nano scale devices, using conventional batteries that lack flexibility and have a short lifetime, presents obstacles to the development of further miniaturization of electronic devices [5, 6]. As an alternative, harvesting energy from the environment with the help of nanogenerators (NGs), has been recently explored to convert abundant natural energy into free electricity through a variety of mechanisms such as piezoelectric, pyroelectric, and photoelectric, electromagnetic phenomenon [7–11]. However, these devices offer lower power output for their respective electrical application, endure less time with continuous mechanical stretching or vibration, and lack adequate flexibility and biocompatibility [12–15].

With this incessant growth and demand for energy, in 2012, Dr. Wang's group introduced triboelectric nanogenerators (TENG) [16]. TENG have been proposed as a new form of energy harvester that can convert frictional force into electrical energy [17, 18]. TENG are promising alternative energy sources and have been named "the energy for the new era" [19–21]. The mechanical contact of two dissimilar materials can exhibit triboelectric effects, and with the abundant choice of combination of materials and their respective structures, there are ample opportunities to evaluate different arrangements of TENG devices and their resultant electrical properties [22–24]. TENGs are classified into four different modes: vertical contact-separation (CS) mode, lateral sliding (LS) mode, single electrode (SE) mode, and freestanding triboelectric (FT) mode. All of them are based on the working principle of the combination of contact electrification and electrostatic effects [25–27].

The output of the TENG greatly depends on the active contact area between the two layers, triboelectric materials [28], and effective TENG structure [29]. The selection of the triboelectric material is the most crucial aspect since the nature of the material

dictates the ease of charge ejection and acceptance between the electrodes [30, 31]. Polymers have been widely used in the different layers of the TENGs due to their mechanical flexibility and corrosion resistance [32], as well as their convenience to manufacture films [33–35], aerogels [36], nanowires [37], and, most recently, nanofibers [38, 39]. Furthermore, surface modification through addition of low-dimension carbon allotropes, such as fullerene, graphene, carbon nanotubes, and multi-walled carbon nanotubes into a TENG, can result in a combination that improves electrical output and creates superior multifunctionality of the device [29, 40, 41]. Multi-walled carbon nanotubes (MWCNT) are beneficial to TENGs due to their excellent electrical, thermal, and mechanical properties alongside with their high surface area and high chemical stability [42, 43].

In this study, we developed a nanofiber-based TENG device using a contact and separation mechanism consisting of two distinct layers. The nanofiber-based mats were developed using the Forcespinning technique. The first layer was made of poly(vinylidene fluoride) (PVDF), whilst the second layer was made of polyurethane (TPU) nanofibers coated with functionalized multi-walled carbon nanotubes (MWCNT). The PVDF layer acted as the negative layer, while the TPU functionalized with MWCNT acted as positive layer, due to the difference in charge density [44, 45]. PVDF has been extensively studied for its TENG potential due its piezoelectric nature, flexibility, and promising mechanical properties [46–50]. PVDF possesses *α, β, γ, δ, and ε* phases. However, only the *β* and *γ* phases exhibit a polar response [51, 52]. In the case of nanofibers, the distinguishable *β* phase can be observed when the polymer molecule is stretched by the strong centrifugal force, yielding high electroactive characteristics such as polarizability and dielectric properties, which can offer upgraded triboelectric performance. Compared to other tribo-positive polymers, TPU NF have shown promising mechanical properties, breathability, stretchability and high frictional surface area, making these NF suitable candidates for TENG components [44, 53–55] TPU has been previously used in TENG in combination with other polymers such as polypropylene [56], polyethylene glycol, and polytetrafluoroethylene [57], as well as other materials like silver nanowires and reduced graphene oxide [58].

Here, both TPU and PVDF nanofiber mats were prepared using the Forcespinning (FS) technique [59, 60]. The TPU nanofibers were then dipped into amino, fluorine and carboxyl functional MWCNT (c-MWCNT) solutions, varying the concentration and dipping period to modify the structural and electrical properties. The c-MWCNT dipped for 12 h showed the most promising interaction with the TPU nanofibers. Consequently c-MWCNT functionalized TPU/PVDF-based triboelectric nanogenerators were further investigated for their triboelectric performance. Additionally, morphological and structural investigations were conducted to assess the uniformity and continuity of the forcespun fibers. The prepared TENG were also assessed to examine their charging capability. The developed TENG showed desired flexibility and biocompatibility with promising potential to be used in wearable devices, such as artificial neural networks (ANN) [61, 62].

Results and discussions

Characterization of the fibers

Figure 1 shows the synthetic process for the production and dipping of the TPU nanofiber mats. Figure 2 exhibits the field emission scanning electron microscopy (FESEM) micrographs of the unmodified TPU and PVDF mats, along with their respective histograms of fiber diameter. Figure 2(a and b) illustrate long, continuous, and uniform fibers for both TPU and PVDF nanofiber mats. The average fiber diameter of TPU and PVDF nanofibers is shown to be 393 and 203 nm, respectively.

The FESEM micrographs in Fig. 3 show the morphology of the bare TPU nanofibers and those coated with functionalized multiwall carbon nanotubes (f-MWCNT). Figure 3(a) shows the untreated TPU nanofiber. Figure 3(b) illustrates the TPU fibers coated with the -NH_2 f-MWCNT it can be observed that the carbon nanotubes are unevenly distributed on the nanofibers, substantial clusters of multi-walled carbon nanotubes are present on the surface of the fibers. Additionally, TPU fibers were also coated with the –F functionalized MWCNT and the resulting micrograph [Fig. 3(c)] reveals clean TPU nanofibers with no trace of MWCNT, indicating that fluorine f-MWCNTs were not successfully dispersed and integrated along the TPU fiber surface. The poor interaction between the TPU fibers and –NH_2 and –F functionalized MWCNT [Fig. 3(b and c)] led to no further development in this study regarding FTIR spectroscopy, XPS and electrical performance testing. Figure 3(d–f) display micrographs of TPU fibers coated with –COOH functionalized MWCNT at different dipping times (6, 12 and 24 h, respectively). It can be elucidated that the dispersion and distribution of c-MWCNT vary over dipping time. For the 6 h dipping time [Fig. 3(d)], the c-MWCNT are more agglomerated in certain areas along the TPU fiber, indicating attachment of MWCNT to the fibers, but poor dispersion and distribution throughout the fiber mat. Upon increasing dipping time to 12 h [Fig. 3(e)], a more uniform dispersion is observed throughout the fiber structure. However, with a 24 h. dipping time [Fig. 3(f)], a detrimental effect was produced as not all areas exhibit the same concentration of f-MWCNT, suggesting that the dispersion in the solution was not constant over time. Consequently, samples with 12 h. dipping with c-MWCNT were selected for the development of the TENG.

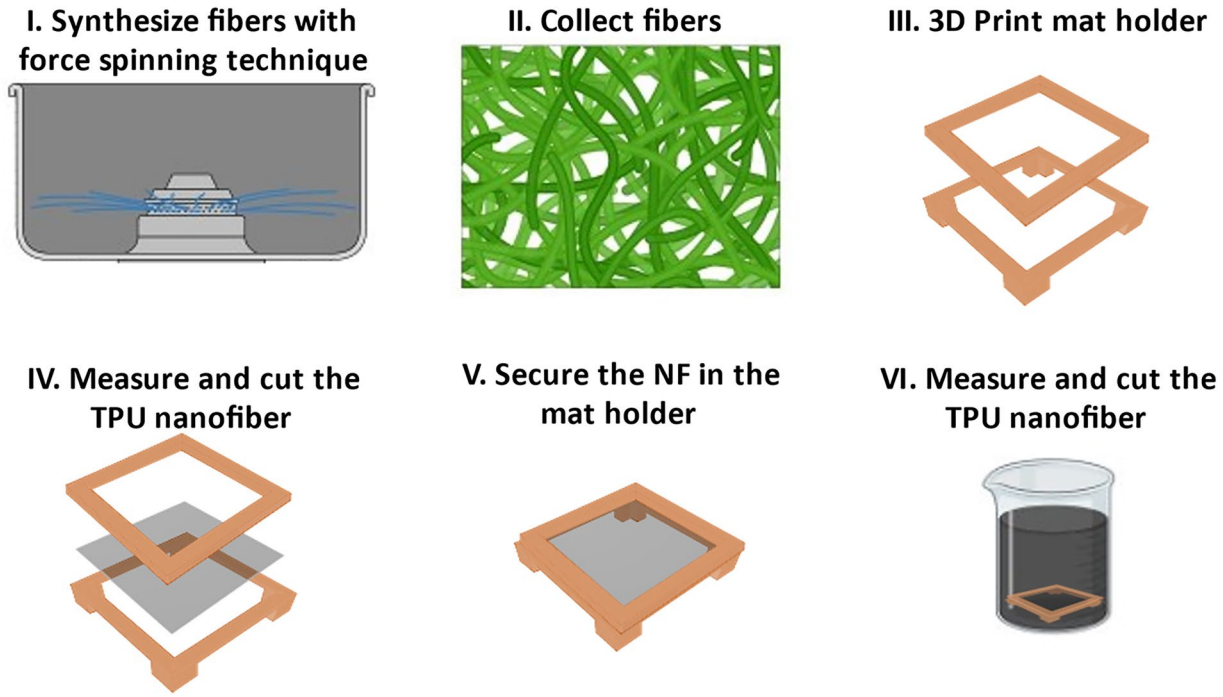

Figure 1: Scheme of NF production and 3D drawing of the mat holder and dipping process.

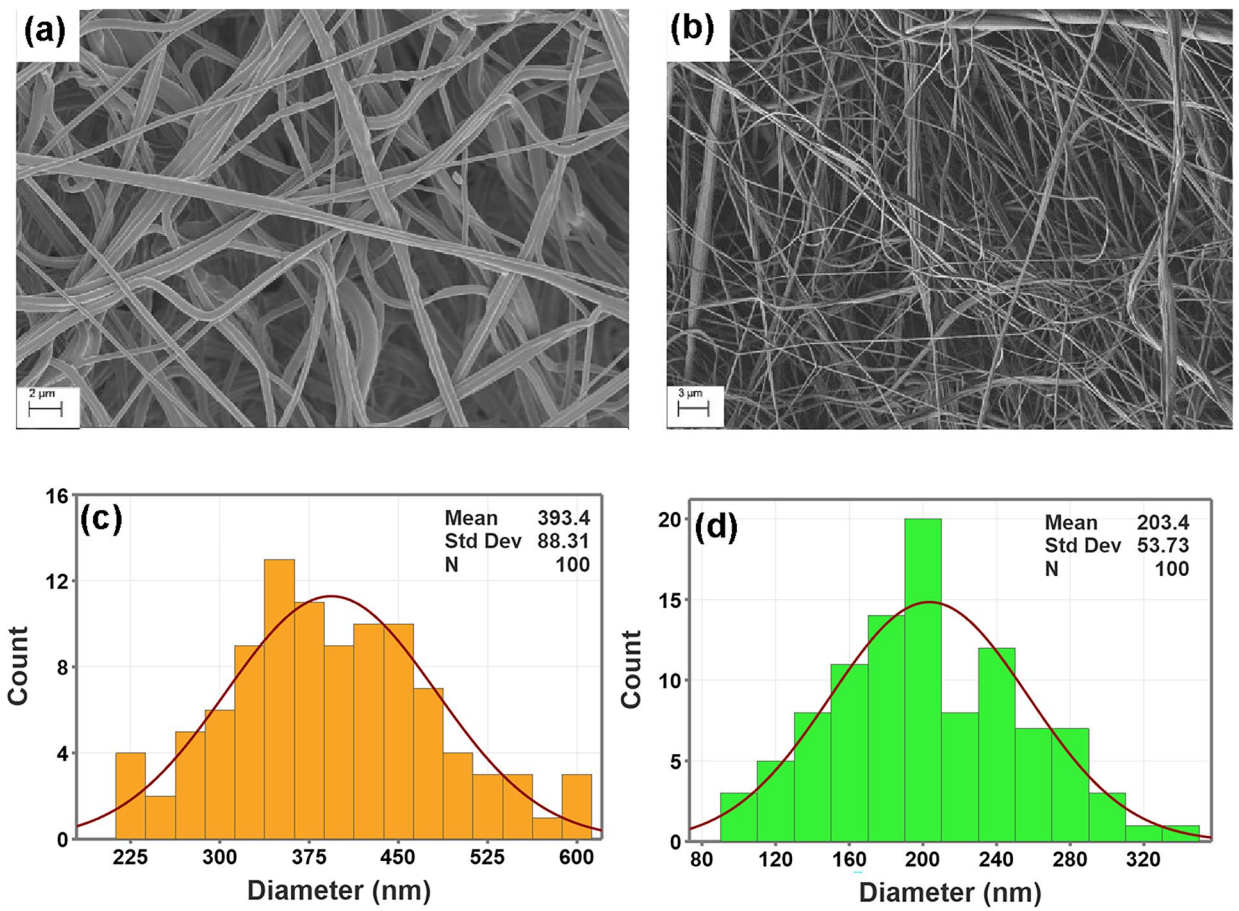

Figure 2: FESEM images of (a) TPU and (b) PVDF; fiber diameter distribution histograms (c) TPU and (d) PVDF.

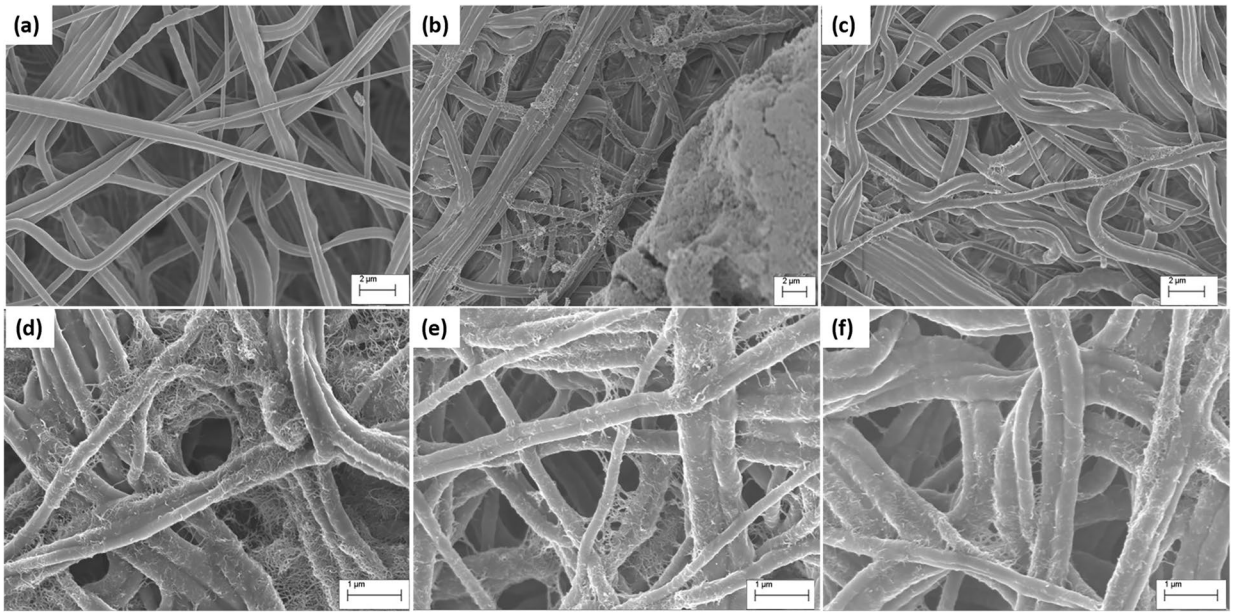

Figure 3: FESEM morphology of TPU nanofibers modified with (a) non-treated, (b) $-NH_2$ f-MWCNT for 24 h (c) –F f-MWCNT for 24 h, (d) –COOH f-MWCNT for 6 h, (e) –COOH f-MWCNT for 12 h and (f) –COOH f-MWCNT for 24 h.

Vibrational spectroscopy

The PVDF and TPU nanofibers were further analyzed using Fourier-transform infrared spectroscopy (FTIR) with the corresponding spectra illustrated in Fig. 4. The characteristic β phase for PVDF nanofibers [Fig. 4(a)] was observed at the wavenumber of 877 cm^{-1}, 1172 cm^{-1} and 1401 cm^{-1}, the stretching at 877 cm^{-1} corresponds to the C–C skeletal vibration of β PVDF while the peaks at 1172 and 1401 cm^{-1} can be attributed to the C–F and C–H stretching vibrations, respectively [63, 64]. The β phase in PVDF significantly contributes to the triboelectric phenomena in the nanogenerator. Apart from these, the peaks at 510 and 839 cm^{-1} resulted from the $-CF_2$ bending and a mixed mode of $-CH_2-$ rocking and $-CF_2-$ asymmetric stretching vibration [64, 65]. From 4b, it can be observed that there are no new absorption peaks between the untreated TPU and the TPU modified with MWCNT with functional –COOH groups. However, differences in absorption intensity are noticeable in all these peaks consistent with comparable results by Arup et al. [66]. The peak observed near 3330 cm^{-1} is related to the N–H stretching vibration in the urethane group, while peaks

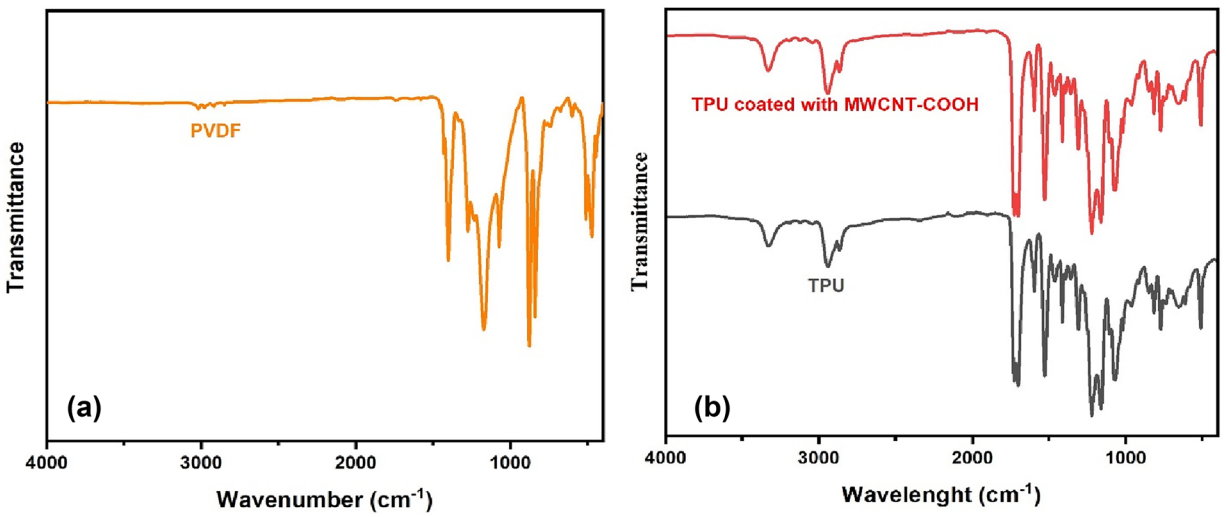

Figure 4: FTIR spectra for (a) PVDF nanofibers, (b) TPU nanofibers and TPU nanofibers coated with MWCNT- COOH.

near 2941 cm^{-1} correspond to—CH_2– asymmetric stretching vibration [67]. Sharp peaks near 1728 cm^{-1} and 1699 cm^{-1} were associated with stretching vibrations of the carbonyl group C=O in the amide, while the peak at 1596 cm^{-1} are attributed to N–H group flexural absorption [68]. The peak near 1411 cm^{-1} is related to the CH_2 asymmetric vibrations, and bands around 1222 cm^{-1} and 1081 cm^{-1} are due to the C–O stretching [69].

X-ray photoelectron spectroscopy

Since FTIR alone was insufficient to confirm the interaction with the c-MWCNT results were complemented with XPS analysis. Figure 5(a) presents the XPS fitting peaks for the Cs1 elements of the non-modified TPU. The distinctive peaks observed at 284.3, 285.5, 285.9 and 288.2, are related to C–C, C–N, C–O and C=O respectively. According to the quantitative results obtained in Fig. 5(b), it was found that the C–C shifted to a lower energy level due to the isolation effect of TPU. Additionally, the C=O bond is much more intense in the modified TPU, attributed to the presence of carboxyl groups present in the c-MWCNT [70, 71].

In Fig. 5(c), XPS peaks from the Os1 elements in the non-modified TPU are shown, with distinctive peaks observed at 531.2 and 532.8 eV related to the C=O and C–O bonds respectively, however in Fig. 5(d) a new peak appears around 533.3 which can be related to O–C=O bond [72]. These results successfully demonstrate surface modification of the TPU NF through the c-MWCNT. This is evidenced by the changes presented in both the carbon and oxygen, elements peaks analyzed, specifically in the change of intensity in the 288.2 eV peak attributed to the C=O bond in Cs1, and the appearance of the 533.3 eV peak related to the O–C=O bond in the element Os1, both of these peaks can be directly attributed to the presence of c-MWCNT on the surface of the TPU fibers.

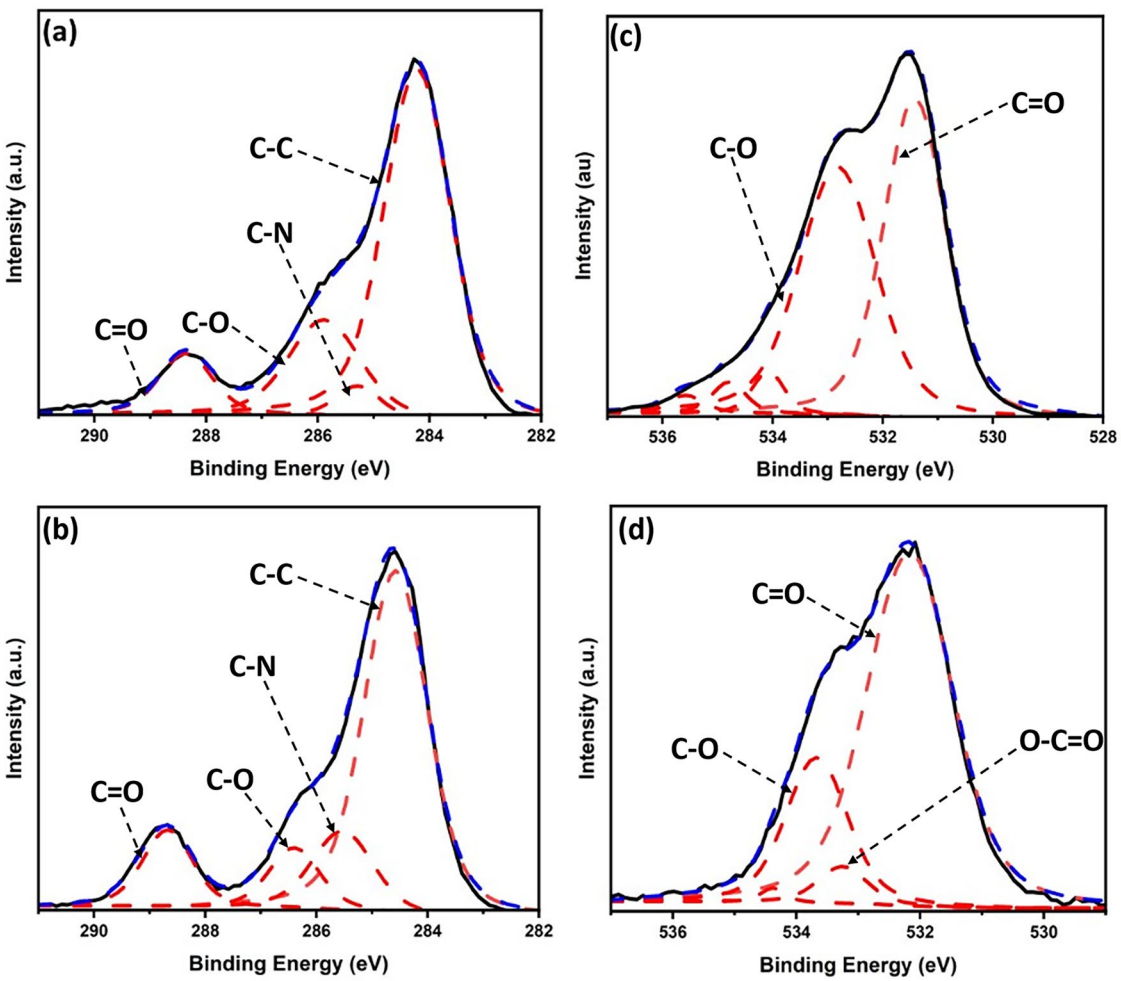

Figure 5: XPS peak fitting of (a) Cs1 non modify TPU NF, (b) Cs1 modified with c-MWCNT/TPU, (c) Os1 non modified TPU NF, (d) Os1 modified with c-MWCNT/TPU.

Electrical performance

The detailed mechanism of PVDF and TPU nanofiber-based triboelectric nanogenerator (vertical contact and separation based TENG) is illustrated in Fig. 6. Initially, the triboelectric pairs initiates in a fully separated mode, where both the TPU (positive electrode) coated with c-MWCNT and the PVDF (negative electrode) are fully separated, resulting in no charge generation and no potential difference between the triboelectric nanofiber layers. The two NF layers were then periodically pressed and separated [Fig. 6(d)], which resulted in the difference in electronegativity between the layers, which leads to charge ejection from the c-MWCNT coated TPU layer to the PVDF nanofiber layer [44]. The electron affinities of the triboelectric materials introduce an equivalent amount of opposite charges between the triboelectric interface, leading to the formation of an electric potential difference [15]. During the releasing mode, an electric potential difference is generated among the triboelectric layers, which urged the free electrons to flow from the PVDF nanofiber to the c-MWCNT coated TPU layer connected via an external load [40]. This results in an instantaneous flow of current, and as the external force is gradually released, the potential difference further increases until the NF layers are fully separated. This process balances the induced potential difference, and the open-circuit voltage (V_{oc}) becomes zero [41]. Once the external force is applied to the tribo-layers and brought closer to each other, the accumulated free charges flowed in the opposite direction, leading to a reversal in electricity flow [73]. Similar to the separated mode, once both layers are completely contacted, the potential difference becomes zero. The oscillating compression and release mechanism results in alternating voltage and current, eventually transforming the external mechanical energy into electricity.

The c-MWCNT embedded TPU/PVDF TENGs were tested using a vertical punch, applying pressures of 10, 15, 20, and 30 psi at a constant frequency of 65 bpm. The results in Fig. 6(e–j) show highly uniform peaks for both open circuit voltage (V_{oc}) and short circuit current (I_{sc}). For the samples dipped for 6 h, the maximum V_{oc} values were 51.2, 72.8, 106 and 128 V and the I_{sc} were 26, 36, 70 and 100 μA for the applied pressures. Similarly, the highest V_{oc} values obtained for the sample dipped for 12 h. were 64, 86, 136, 158 V, while for 24 h, the recorded results were 32, 50.8, 76, 112 V. Additionally, the maximum I_{sc} obtained for the 12 h. dipped c-MWCNT f-TPU/PVDF TENG were 48, 66, 114, and 170 μA while for the samples dipped for 24 h., the results were 36, 54, 96, and 118 μA. As the pressure increased, both V_{oc} and I_{sc} were increased [7, 44], though for each case (V_{oc} and I_{sc}), the maximum output was observed for the samples dipped for 12 h. As shown above, this dipping time showed the best dispersion and distribution of the functionalized c-MWCNT.

In summary, the increase in load on a TENG refers to either applying an external load or connecting the TENG to a circuit to extract power from it. When the load on a TENG increases, two main factors contribute to the increased open-circuit voltage and short-circuit current: enhanced charge transfer and increased mechanical deformation with a higher load. As the load increases, the TENG experiences greater mechanical deformation and a larger contact area between the triboelectric materials, leading to enhanced charge transfer during the triboelectrification process. This results in a larger charge separation, leading to a higher open-circuit voltage, which is the voltage generated by the TENG when it is not connected to any external circuit.

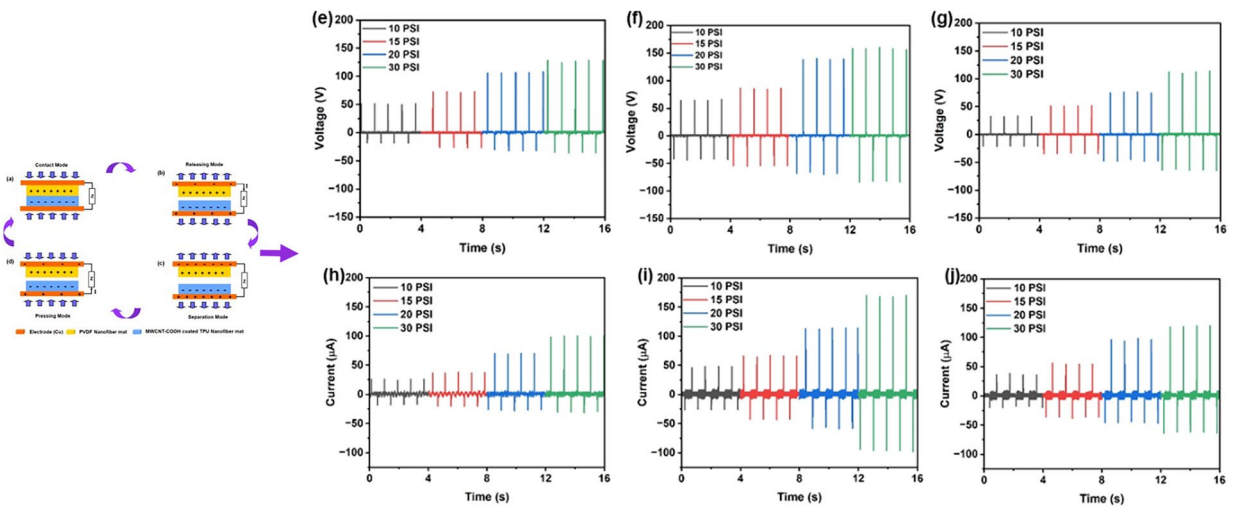

Figure 6: (a–d) Operating mechanism of NF based TENG Electrical performance of NF-TENG. (e–g) Open circuit voltage (V_{oc}) and (h–j) Short circuit current (I_{sc}) current of the TENG at different pressures for TPU nanofibers dipped in c-MWCNT for (e, h) 6 h, (f, i) 12 h, (g, j) 24 h, respectively.

Improved transport charge was observed, as the load on the TENG increases, the extracted current also increases. This is because a higher load creates a lower impedance path for the flow of charge carriers (electrons) from the TENG. The lower impedance allows for improved charge transport, resulting in a higher short circuit current, which is the current generated when the TENG is connected to a short circuit.

From Fig. 7(a) it is evident that the peak-to-peak voltage output of NF-based TENGs was 69.6, 99.2, 138, and 164 V (for 6 h. dipping); 106, 140, 206, and 242 V (for 12 h. dipping) and 52.8, 84.8, 124, and 176 V (for 24 h. dipping) at 10, 15, 20, 30 psi, respectively. Similarly, the alternating peak-to-peak current output shows similar trend, with recorded outputs of 44, 56, 96, and 130 μA (for 6 h. dipping); 74, 108, 172, and 266 μA (for 12 h. dipping) and 56, 90, 142, and 180 μA (for 24 h. dipping) at 10, 15, 20, 30 psi, respectively. The maximum peak-to-peak value was obtained for each case at 30 Psi, with the highest value achieved for the 12 h. dipping condition [Fig. 7(b)]. However, after 12 h. dipping the maximum peak-to-peak voltage and current output decreased. It is important to note that this peak-to-peak data represents a load frequency of 65 for varied pressure from 10 to 30 psi, and the active area of the sample was the same for all cases at 0.7854 in^2. Furthermore, three NF TENGs (TPU NF dipped at 6, 12, 24 h.) were tested, while connected with a 1 μF capacitor, by hand tapping motion, yielding a charge of 2.91, 3.03, and 2.49 V for the fibers dipped for 6, 12 and 24 h, respectively, with only 25 s of tapping at 240 bpm or 4 Hz load frequency. This charging capability demonstrates the potential application of the developed TENG as self-charging energy harvesters with sensor related applications.

Conclusions

In this study, triboelectric nanogenerators were proposed and fabricated using PVDF and TPU nanofibers synthesized via the forcespinning technique. Developed TPU nanofiber mats were coated with c-MWCNT through a dipping process to modify their surface. Fibers were dipped for 6, 12 and 24 h, with 12 h resulting in better dispersion of the c-MWCNT along the TPU fiber surface. The resulting nanofiber-based TENG exhibited a high alternating voltage signal, attributed to the increased beta phase of the PVDF and the surface modification of TPU. TENGs were evaluated using a cylindrical pneumatic punch machine with a range of pressure (10, 15, 20 and 30 psi) at a load frequency of 65 BPM (beats per minute) to obtain uniform electrical voltage and current output. The TENG with the TPU nanofiber dipped for 12 h demonstrated the most effectiveness, with the maximum open-circuit voltage and short-circuit current reported as 158 V and 170 µA, respectively. The TENG charging capacity for the samples dipped for 12 h showed an ability to charge a 1 µF capacitor to 3.03 V in only 25 s of hand tapping. In summary, we fabricated fully NF based TENG and demonstrated a modification procedure of the triboelectric layer, which holds the potential for use in flexible and stretchable self-charging energy harvesting device.

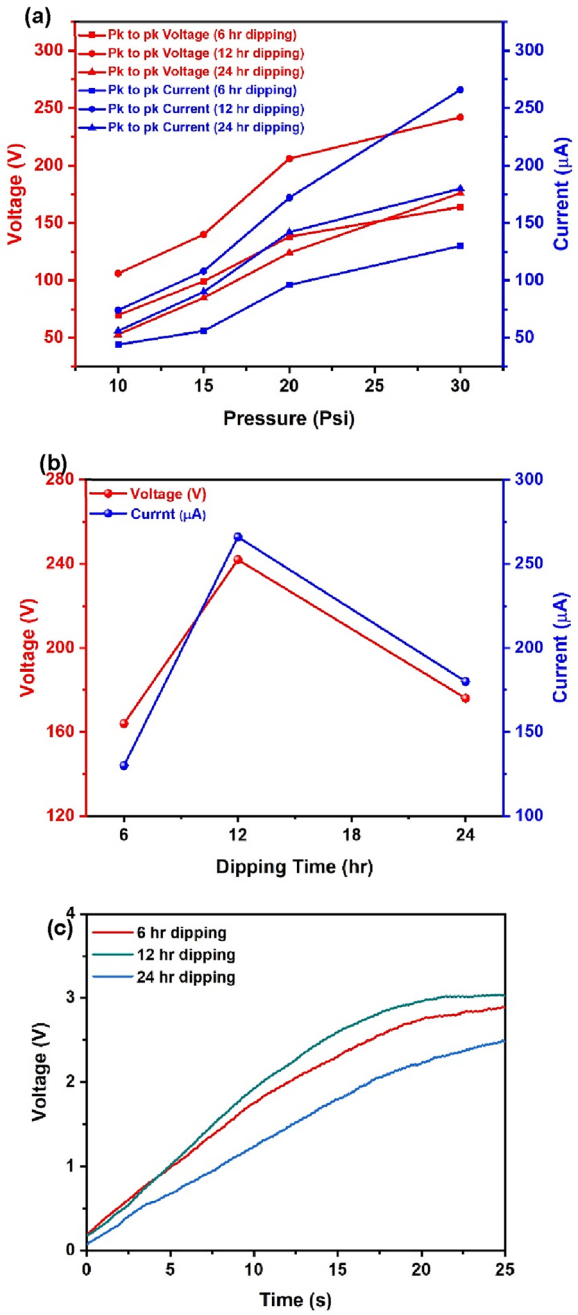

Figure 7: (a) Peak-to-peak voltage and current output of the TENG at different pressures, (b) Maximum peak-to-peak voltage and current output for TPU nanofibers dipped in c-MWCNT and (c) Charging ability of NF based TENG with 1 μF capacitor for 6, 12 and 24 h, respectively.

Experimental section

Materials

Acetone (HPLC, ≥ 99.9%), COOH functionalized multi-walled carbon nanotubes, poly [4,4′-methylenebis (phenyl isocyanate)-alt-1,4-butanediol/di(propylene glycol)/poly caprolactone], and methylene-diisocyanate (MDI) thermoplastic polyester/polyether polyurethane (TPU), were all purchased from Sigma-Aldrich. NH_2 functionalized multi-walled carbon nanotubes and F functionalized multi-walled carbon nanotubes were obtained from Cheaptubes. The KYNAR 741 poly(vinylidene fluoride) (PVDF) powder was purchased from Arkema Inc. Ethyl alcohol, N,N-dimethylformamide (DMF, ≥ 99.7%), and dimethylacetamide (DMA, C4H9NO) were all acquired from Fisher Scientific.

Preparation of PVDF and TPU nanofiber mats

Nanofibers were synthesized from polymer solutions. For the PVDF polymer solution, PVDF (1.1 g) was dissolved into a mixture of DMA (2.35 g) and acetone (1.96 g) in a 20 mL scintillation vial. The PVDF polymer solution was then placed onto a silica oil bath at 60 °C and magnetically stirred at 800 rpm for 24 h. Similarly, a 16 wt% TPU polymer solution was obtained by dissolving it in DMF solvent. The solution was placed in a silica oil bath at 105 °C and continuously stirred magnetically at 1000 rpm for 48 h. After complete homogenization, the solution was removed and allowed to cool at room temperature.

The Cyclone L-1000 system (Fiberio Technology Corp) utilizing Forcespinning technology was employed to produce nanofiber mats. Upon cooling the solution, 2 mL polymer solution was injected into a spinneret equipped with 30-gauge precision needles. An aluminum collector was utilized to retrieve the initial batch of non-woven nanofibers, and after five iterations, a nanofiber mat was collected for both cases.

Preparation of dipping solution

Three separated dipping solutions were prepared, one for each functionalized MWCNT (–COOH, –F, –NH2) These solutions were prepared in a beaker containing a 5 wt% of acetone and 0.01 wt% of the respective MWCNT, using ethanol as the solvent The dipping solutions were sonicated (Q700 Sonicator with Standard 4220 Probe) for 10 min with a three-second interval of sonication and non-sonication with an amplitude of 40. The solution was then kept under continuous magnetic stirring to ensure homogeneity.

Dipping process

Initially the mat holder was 3D printed which consisted of a top and bottom frame. The TPU fiber mat was placed in between these two frames and secured with a pair of zip ties to prevent crumpling and fix the mat in place. The mat holder was then submerged in the dipping solution. The solution with the mat holder was magnetically stirred at 60 rpm for 6, 12, 24 h. Afterwards, the mats were washed with distilled water from both sides and left on the holder to air dry for 3 h and subsequently oven dried for 6 h at 60 °C to obtain functionalized MWCNT (f-MWCNT) coated TPU fiber mat.

Fabrication of triboelectric nanogenerator (TENG) device

Square mats of 1.5×1.5 in^2 were cut from both the PVDF nanofibers and f-MWCNT coated TPU nanofibers to fabricate the TENG. Samples were adhered to copper tape (0.06 mm thick) of equivalent area. The two layers were separated with the inclusion of two PU spacers (1.5×0.2 in^2). Cardboard was used as structural support and placed on top of the copper tape.

Characterization of morphology

The morphology of the f-MWCNT coated TPU nanofibers was characterized using a field emission scanning electron microscope (FESEM) with parameters of acceleration voltage between 2 and 3 kV, with different magnifications (Sigma VP, Carl Zeiss, Jena, Germany). The Fourier transform infrared spectra (FTIR) characterization of PVDF and -COOH functionalized MWCNT coated TPU nanofibers were performed using a 133 VERTEX 70v FTIR Spectrometer (Bruker) in attenuated total reflection (ATR) mode, and the transmittance data of the nanofibers recorded from 450 cm^{-1} to 4000 cm^{-1}. The X-ray photoelectron spectra (XPS) characterization of the TPU –COOH MWCNT was conducted using a K-Alpha Surface Analysis, advantage v5.9922.

Characterization of electrical properties

A Tektronix TDS1001B digital oscilloscope was used to characterize the open-circuit output voltage of the TENG, this oscilloscope has a specified input resistance of 1 MΩ in parallel with approximately 18 pF of input capacitance, while the short-circuit current was measured by the connection of the oscilloscope to the Stanford Research Systems SR570 current preamplifier. For charging capacity tests, the output voltage was measured using a Versa STAT 3 potentiostat, while electrical connectors were attached to the nanogenerator electrodes.

Acknowledgments

The authors gratefully acknowledge the support received by the US National Science Foundation (NSF) award under grant No. DMR- 2122178 UTRGV-UMN Partnership to Strengthen

the PREM Pathway. MJU acknowledges the support from Welch Foundation Grant (2022-2025; BX 0048). The authors declare no conflict of interest.

Author contributions

The manuscript was written by Sk. Shamim Hasan Abir and Julia I. Salas. The experiments and characterizations were performed by Julia I. Salas, Diego de Leon, Ignacio Serrato III. The manuscript was reviewed and edited by Horacio Vasquez, Karen Lozano, and M. Jasim Uddin. The project was supervised by Karen Lozano and M. Jasim Uddin. The project was conceptualized by M. Jasim Uddin. All the authors have given their approval to the last version of the manuscript.

Funding

The project is under the US National Science Foundation (NSF) award under grant No. DMR- 2122178 UTRGV-UMN Partnership to Strengthen the PREM Pathway. MJU acknowledges the support from Welch Foundation Grant (2022-2025; BX 0048).

Data availability

The data is available upon request.

Declarations

Competing interests The authors declare that they have no known competing financial interests or personal relationships that could have appeared to influence the work reported in this paper.

Supplementary Information

The online version contains supplementary material available at https://doi.org/10.1557/s43578-024-01368-8.

References

1. S. Shrivastava, T.Q. Trung, N.E. Lee, Recent progress, challenges, and prospects of fully integrated mobile and wearable point-of-care testing systems for self-testing. Chem. Soc. Rev. (2020). https://doi.org/10.1039/c9cs00319c
2. J. Kim, R. Kumar, A.J. Bandodkar, J. Wang, Advanced materials for printed wearable electrochemical devices: a review. Adv. Electron. Mater. (2017). https://doi.org/10.1002/aelm.201600260
3. H.R. Lim, H.S. Kim, R. Qazi, Y.T. Kwon, J.W. Jeong, W.H. Yeo, Advanced soft materials, sensor integrations, and applications of wearable flexible hybrid electronics in healthcare, energy, and environment. Adv. Mater. (2020). https://doi.org/10.1002/adma.201901924
4. J.H. Lee, H. Chen, E. Kim, H. Zhang, K. Wu, H. Zhang, X. Shen, Q. Zheng, J. Yang, S. Jeon, J.K. Kim, Flexible temperature sensors made of aligned electrospun carbon nanofiber films with outstanding sensitivity and selectivity towards temperature. Mater. Horizons. (2021). https://doi.org/10.1039/d1mh00018g
5. B. Kang, G. Ceder, Battery materials for ultrafast charging and discharging. Nature (2009). https://doi.org/10.1038/nature07853
6. C.K. Chan, H. Peng, G. Liu, K.M. Ilwrath, X.F. Zhang, R.A. Huggins, Y. Cui, High-Performance Lithium Battery Anodes Using Silicon Nanowires, in *Materials for Sustainable Energy: A Collection of Peer-Reviewed Research and Review Articles from Nature Publishing Group*. ed. by V. Dusastre (Macmillan Publishers Ltd, New York, 2010)
7. S.S.H. Abir, J.E. Trevino, B.B. Srivastava, M.U.K. Sadaf, J.I. Salas, K. Lozano, M.J. Uddin, Synthesis of color tunable piezoelectric nanogenerators using CsPbX3 perovskite nanocrystals embedded in poly(D, L-lactide) membranes. Nano Energy **102**, 107674 (2022). https://doi.org/10.1016/j.nanoen.2022.107674
8. E. Islam, A.M. Abdullah, A.R. Chowdhury, F. Tasnim, M. Martinez, C. Olivares, K. Lozano, M.J. Uddin, Electromagnetic-triboelectric-hybrid energy tile for biomechanical green energy harvesting. Nano Energy (2020). https://doi.org/10.1016/j.nanoen.2020.105250
9. D.P. Arnold, Review of microscale magnetic power generation. IEEE Trans. Magn. (2007). https://doi.org/10.1109/TMAG.2007.906150
10. H. Askari, N. Xu, B.H. Groenner Barbosa, Y. Huang, L. Chen, A. Khajepour, H. Chen, Z.L. Wang, Intelligent systems using triboelectric, piezoelectric, and pyroelectric nanogenerators. Mater. Today (2022). https://doi.org/10.1016/j.mattod.2021.11.027
11. W. Ma, R. Zhu, L. Rufer, Y. Zohar, M. Wong, An integrated floating-electrode electric microgenerator. J. Microelectromech. Syst. (2007). https://doi.org/10.1109/JMEMS.2006.885856
12. C. Jiang, C. Wu, X. Li, Y. Yao, L. Lan, F. Zhao, Z. Ye, Y. Ying, J. Ping, All-electrospun flexible triboelectric nanogenerator based on metallic MXene nanosheets. Nano Energy **59**, 268–276 (2019). https://doi.org/10.1016/j.nanoen.2019.02.052
13. C. Qian, L. Li, M. Gao, H. Yang, Z. Cai, B. Chen, Z. Xiang, Z. Zhang, Y. Song, All-printed 3D hierarchically structured cellulose aerogel based triboelectric nanogenerator for multi-functional sensors. Nano Energy (2019). https://doi.org/10.1016/j.nanoen.2019.103885
14. J.G. Sun, T.N. Yang, C.Y. Wang, L.J. Chen, A flexible transparent one-structure tribo-piezo-pyroelectric hybrid energy generator based on bio-inspired silver nanowires network for biomechanical energy harvesting and physiological monitoring. Nano Energy (2018). https://doi.org/10.1016/j.nanoen.2018.03.071
15. Y. Zhu, B. Yang, J. Liu, X. Wang, L. Wang, X. Chen, C. Yang, A flexible and biocompatible triboelectric nanogenerator with

tunable internal resistance for powering wearable devices. Sci. Rep. **6**, 1–10 (2016). https://doi.org/10.1038/srep22233

16. Z.L. Wang, Triboelectric nanogenerator (TENG)—sparking an energy and sensor revolution. Adv. Energy Mater. (2020). https://doi.org/10.1002/aenm.202000137
17. F.R. Fan, Z.Q. Tian, Z. Lin Wang, Flexible triboelectric generator. Nano Energy **1**, 328–334 (2012). https://doi.org/10.1016/j.nanoen.2012.01.004
18. G.Q. Gu, C.B. Han, J.J. Tian, T. Jiang, C. He, C.X. Lu, Y. Bai, J.H. Nie, Z. Li, Z.L. Wang, Triboelectric nanogenerator enhanced multilayered antibacterial nanofiber air filters for efficient removal of ultrafine particulate matter. Nano Res. **11**, 4090–4101 (2018). https://doi.org/10.1007/s12274-018-1992-1
19. T. Cheng, Q. Gao, Z.L. Wang, The current development and future outlook of triboelectric nanogenerators: a survey of literature. Adv. Mater. Technol. (2019). https://doi.org/10.1002/admt.201800588
20. B. Chen, Y. Yang, Z.L. Wang, Scavenging wind energy by triboelectric nanogenerators. Adv. Energy Mater. (2018). https://doi.org/10.1002/aenm.201702649
21. Z.L. Wang, T. Jiang, L. Xu, Toward the blue energy dream by triboelectric nanogenerator networks. Nano Energy (2017). https://doi.org/10.1016/j.nanoen.2017.06.035
22. C. Wu, A.C. Wang, W. Ding, H. Guo, Z.L. Wang, Triboelectric nanogenerator: a foundation of the energy for the new era. Adv. Energy Mater. (2019). https://doi.org/10.1002/aenm.201802906
23. D. Lopez, A.R. Chowdhury, A.M. Abdullah, M.U.K. Sadaf, I. Martinez, B.D. Choudhury, S. Danti, C.J. Ellison, K. Lozano, M.J. Uddin, Polymer based triboelectric nanogenerator for cost-effective green energy generation and implementation of surface-charge engineering. Energy Technol. (2021). https://doi.org/10.1002/ente.202001088
24. J.I. Salas, D. de Leon, S.S.H. Abir, M.J. Uddin, K. Lozano, Functionalized thermoplastic polyurethane nanofibers: an innovative triboelectric energy generator. Electron. Mater. **4**, 158–167 (2023). https://doi.org/10.3390/electronicmat4040014
25. G. Khandelwal, N.P.M. Joseph Raj, S.J. Kim, Materials beyond conventional triboelectric series for fabrication and applications of triboelectric nanogenerators. Adv. Energy Mater. (2021). https://doi.org/10.1002/aenm.202101170
26. A. Ahmed, I. Hassan, M.F. El-Kady, A. Radhi, C.K. Jeong, P.R. Selvaganapathy, J. Zu, S. Ren, Q. Wang, R.B. Kaner, Integrated triboelectric nanogenerators in the era of the internet of things. Adv. Sci. (2019). https://doi.org/10.1002/advs.201802230
27. J. Luo, Z.L. Wang, Recent progress of triboelectric nanogenerators: From fundamental theory to practical applications. EcoMat. (2020). https://doi.org/10.1002/eom2.12059
28. Z.L. Wang, A.C. Wang, On the origin of contact-electrification. Mater. Today (2019). https://doi.org/10.1016/j.mattod.2019.05.016
29. K. Cheng, S. Wallaert, H. Ardebili, A. Karim, Advanced triboelectric nanogenerators based on low-dimension carbon materials: a review. Carbon (2022). https://doi.org/10.1016/j.carbon.2022.03.037
30. Y. Wang, Y. Yang, Z.L. Wang, Triboelectric nanogenerators as flexible power sources. Npj Flex. Electron. **1**, 1–9 (2017). https://doi.org/10.1038/s41528-017-0007-8
31. Q. Shi, T. He, C. Lee, More than energy harvesting—combining triboelectric nanogenerator and flexible electronics technology for enabling novel micro-/nano-systems. Nano Energy (2019). https://doi.org/10.1016/j.nanoen.2019.01.002
32. B. Yu, H. Yu, T. Huang, H. Wang, M. Zhu, A biomimetic nanofiber-based triboelectric nanogenerator with an ultrahigh transfer charge density. Nano Energy **48**, 464–470 (2018). https://doi.org/10.1016/j.nanoen.2018.03.064
33. A.M. Abdullah, A. Flores, A.R. Chowdhury, J. Li, Y. Mao, M.J. Uddin, Synthesis and fabrication of self-sustainable triboelectric energy case for powering smart electronic devices. Nano Energy **73**, 104774 (2020). https://doi.org/10.1016/j.nanoen.2020.104774
34. D. Zamora, A.M. Abdullah, A. Flores, H. Majumder, M.U.K. Sadaf, B. Azimi, S. Danti, M.J. Uddin, Flexible bielectrode based highly sensitive triboelectric motion sensor: a sustainable and smart electronic material. Energy Technol. (2022). https://doi.org/10.1002/ente.202100662
35. A.R. Chowdhury, A.M. Abdullah, I. Hussain, J. Lopez, D. Cantu, S.K. Gupta, Y. Mao, S. Danti, M.J. Uddin, Lithium doped zinc oxide based flexible piezoelectric-triboelectric hybrid nanogenerator. Nano Energy **61**, 327–336 (2019). https://doi.org/10.1016/j.nanoen.2019.04.085
36. Q. Zheng, L. Fang, H. Guo, K. Yang, Z. Cai, M.A.B. Meador, S. Gong, Highly porous polymer aerogel film-based triboelectric nanogenerators. Adv. Funct. Mater. (2018). https://doi.org/10.1002/adfm.201706365
37. S. Cui, Y. Zheng, J. Liang, D. Wang, Conducting polymer PPy nanowire-based triboelectric nanogenerator and its application for self-powered electrochemical cathodic protection. Chem. Sci. (2016). https://doi.org/10.1039/c6sc02562e
38. X. Zhang, S. Lv, X. Lu, H. Yu, T. Huang, Q. Zhang, M. Zhu, Synergistic enhancement of coaxial nanofiber-based triboelectric nanogenerator through dielectric and dispersity modulation. Nano Energy (2020). https://doi.org/10.1016/j.nanoen.2020.104894
39. S. Jang, H. Kim, Y. Kim, B.J. Kang, J.H. Oh, Honeycomb-like nanofiber based triboelectric nanogenerator using self-assembled electrospun poly(vinylidene fluoride-co-trifluoroethylene) nanofibers. Appl. Phys. Lett. (2016). https://doi.org/10.1063/1.4945329
40. X. Wang, B. Yang, J. Liu, Y. Zhu, C. Yang, Q. He, A flexible triboelectric-piezoelectric hybrid nanogenerator based on P(VDF-TrFE) nanofibers and PDMS/MWCNT for wearable devices. Sci. Rep. **6**, 1–10 (2016). https://doi.org/10.1038/srep36409
41. N. Sun, G.G. Wang, H.X. Zhao, Y.W. Cai, J.Z. Li, G.Z. Li, X.N. Zhang, B.L. Wang, J.C. Han, Y. Wang, Y. Yang, Waterproof,

breathable and washable triboelectric nanogenerator based on electrospun nanofiber films for wearable electronics. Nano Energy **90**, 106639 (2021). https://doi.org/10.1016/j.nanoen.2021.106639

42. S.Y. Wu, Y.L. Huang, C.C.M. Ma, S.M. Yuen, C.C. Teng, S.Y. Yang, C.H. Twu, Mechanical, thermal and electrical properties of multi-walled carbon nanotube/aluminium nitride/polyetherimide nanocomposites. Polym. Int. (2012). https://doi.org/10.1002/pi.4184
43. B.I. Kharisov, O.V. Kharissova, Carbon allotropes: metal-complex chemistry. Prop. Appl. (2019). https://doi.org/10.1007/978-3-030-03505-1
44. S.S.H. Abir, M.U.K. Sadaf, S.K. Saha, A. Touhami, K. Lozano, M.J. Uddin, Nanofiber-based substrate for a triboelectric nanogenerator: high-performance flexible energy fiber mats. ACS Appl. Mater. Interfaces **13**, 60401–60412 (2021). https://doi.org/10.1021/acsami.1c17964
45. Polymer Materials for High-Performance Triboelectric Nanogenerators.pdf, (n.d.).
46. J.P. Lee, J.W. Lee, J.M. Baik, The progress of PVDF as a functional material for triboelectric nanogenerators and self-powered sensors. Micromachines. (2018). https://doi.org/10.3390/mi9100532
47. K. Xia, Z. Zhu, H. Zhang, Z. Xu, A triboelectric nanogenerator as self-powered temperature sensor based on PVDF and PTFE. Appl. Phys. A Mater. Sci. Process. (2018). https://doi.org/10.1007/s00339-018-1942-5
48. S.M.S. Rana, M.T. Rahman, M. Salauddin, S. Sharma, P. Maharjan, T. Bhatta, H. Cho, C. Park, J.Y. Park, Electrospun PVDF-TrFE/MXene nanofiber mat-based triboelectric nanogenerator for smart home appliances. ACS Appl. Mater. Interfaces (2021). https://doi.org/10.1021/acsami.0c17512
49. X. Pu, J.W. Zha, C.L. Zhao, S.B. Gong, J.F. Gao, R.K.Y. Li, Flexible PVDF/nylon-11 electrospun fibrous membranes with aligned ZnO nanowires as potential triboelectric nanogenerators. Chem. Eng. J. **398**, 125526 (2020). https://doi.org/10.1016/j.cej.2020.125526
50. Y. Kim, X. Wu, C. Lee, J.H. Oh, Characterization of PI/PVDF-TrFE composite nanofiber-based triboelectric nanogenerators depending on the type of the electrospinning system. ACS Appl. Mater. Interfaces (2021). https://doi.org/10.1021/acsami.1c04450
51. T. Bhatta, P. Maharjan, H. Cho, C. Park, S.H. Yoon, S. Sharma, M. Salauddin, M.T. Rahman, S.S. Rana, J.Y. Park, High-performance triboelectric nanogenerator based on MXene functionalized polyvinylidene fluoride composite nanofibers. Nano Energy **81**, 105670 (2021). https://doi.org/10.1016/j.nanoen.2020.105670
52. K. Ke, P. Pötschke, D. Jehnichen, D. Fischer, B. Voit, Achieving β-phase poly(vinylidene fluoride) from melt cooling: effect of surface functionalized carbon nanotubes. Polymer **55**, 611–619 (2014). https://doi.org/10.1016/j.polymer.2013.12.014
53. L.D. Tijing, C.H. Park, W.L. Choi, M.T.G. Ruelo, A. Amarjargal, H.R. Pant, I.T. Im, C.S. Kim, Characterization and mechanical performance comparison of multiwalled carbon nanotube/polyurethane composites fabricated by electrospinning and solution casting. Compos. Part B Eng. **44**, 613–619 (2013). https://doi.org/10.1016/j.compositesb.2012.02.015
54. N. Shehata, R. Nair, R. Boualayan, I. Kandas, A. Masrani, E. Elnabawy, N. Omran, M. Gamal, A.H. Hassanin, Stretchable nanofibers of polyvinylidenefluoride (PVDF)/thermoplastic polyurethane (TPU) nanocomposite to support piezoelectric response via mechanical elasticity. Sci. Rep. **12**, 1–11 (2022). https://doi.org/10.1038/s41598-022-11465-5
55. M. Aurilia, F. Piscitelli, L. Sorrentino, M. Lavorgna, S. Iannace, Detailed analysis of dynamic mechanical properties of TPU nanocomposite: the role of the interfaces. Eur. Polym. J. (2011). https://doi.org/10.1016/j.eurpolymj.2011.01.005
56. H.J. Oh, J.H. Bae, Y.K. Park, J. Song, D.K. Kim, W. Lee, M. Kim, K.J. Heo, Y. Kim, S.H. Kim et al., A highly porous nonwoven thermoplastic polyurethane/polypropylene-based triboelectric nanogenerator for energy harvesting by human walking. Polymers **12**, 1044 (2020). https://doi.org/10.3390/polym12051044
57. H.L. Wang, Z.H. Guo, G. Zhu, X. Pu, Z.L. Wang, ACS Nano **15**(4), 7513–7521 (2021). https://doi.org/10.1021/acsnano.1c00914
58. K. Zhou, Y. Zhao, X. Sun, Z. Yuan, G. Zheng, K. Dai, L. Mi, C. Pan, C. Liu, C. Shen, Ultra-stretchable triboelectric nanogenerator as high-sensitive and self-powered electronic skins for energy harvesting and tactile sensing. Nano Energy **70**, 2211–2855 (2020). https://doi.org/10.1016/j.nanoen.2020.104546
59. E. Ibrahim, S. Ahmed, S.S.H. Abir, K. Taylor, V.M. Padilla-Gainza, K. Lozano, Centrifugally spun alginate-poly(lactic acid) microbeads: a promising carrier for drug delivery and tissue engineering. Int. J. Biol. Macromol. **220**, 671–682 (2022). https://doi.org/10.1016/j.ijbiomac.2022.08.097
60. S.S.H. Abir, M.T. Hasan, M. Alcoutlabi, K. Lozano, The effect of solvent and molecular weight on the morphology of centrifugally spun poly(vinylpyrrolidone) nanofibers. Fibers Polym. (2021). https://doi.org/10.1007/s12221-021-1059-x
61. Y. Liu, L. Wang, D. Li et al., State-of-health estimation of lithium-ion batteries based on electrochemical impedance spectroscopy: a review. Prot. Control Mod. Power Syst. **8**, 41 (2023). https://doi.org/10.1186/s41601-023-00314-w
62. J. Gao, D. Yang, S. Wang, Z. Li, L. Wang, K. Wang, State of health estimation of lithium-ion batteries based on Mixers-bidirectional temporal convolutional neural network. J. Energy Storage. **73**, 109248 (2023). https://doi.org/10.1016/j.est.2023.109248
63. W. Wu, X. Zhang, L. Qin, X. Li, Q. Meng, C. Shen, G. Zhang, Enhanced MPBR with polyvinylpyrrolidone-graphene oxide/PVDF hollow fiber membrane for efficient ammonia nitrogen wastewater treatment and high-density Chlorella cultivation.

Chem. Eng. J. **379**, 122368 (2020). https://doi.org/10.1016/j.cej.2019.122368

64. W. Yang, Y. Li, L. Feng, Y. Hou, S. Wang, B. Yang, X. Hu, W. Zhang, S. Ramakrishna, GO/Bi_2S_3 doped PVDF/TPU nanofiber membrane with enhanced photothermal performance. Int. J. Mol. Sci. **21**, 1–13 (2020). https://doi.org/10.3390/ijms21124224
65. S. Lanceros-Méndez, J.F. Mano, A.M. Costa, V.H. Schmidt, FTIR and DSC studies of mechanically deformed β-PVDF films. J. Macromol. Sci. Phys. **40**, 517–527 (2001). https://doi.org/10.1081/MB-100106174
66. A. Choudhury, P. Kar, Doping effect of carboxylic acid group functionalized multi-walled carbon nanotube on polyaniline. Compos. B Eng. (2011). https://doi.org/10.1016/j.compositesb.2011.04.005
67. A. Asefnejad, M.T. Khorasani, A. Behnamghader, B. Farsadzadeh, S. Bonakdar, Manufacturing of biodegradable polyurethane scaffolds based on polycaprolactone using a phase separation method: physical properties and in vitro assay. Int. J. Nanomedicine **6**, 2375–2384 (2011). https://doi.org/10.2147/ijn.s15586
68. E. Fallahiarezoudar, M. Ahmadipourroudposht, A. Idris, N.M. Yusof, Optimization and development of maghemite (γ-Fe2O3) filled poly-L-lactic acid (PLLA)/thermoplastic polyurethane (TPU) electrospun nanofibers using Taguchi orthogonal array for tissue engineering heart valve. Mater. Sci. Eng. C **76**, 616–627 (2017). https://doi.org/10.1016/j.msec.2017.03.120
69. J.W. Li, H.T. Lee, H.A. Tsai, M.C. Suen, C.W. Chiu, Synthesis and properties of novel polyurethanes containing long-segment fluorinated chain extenders. Polymers (2018). https://doi.org/10.3390/POLYM10111292
70. H.Y. Mi, M.R. Salick, X. Jing, W.C. Crone, X.F. Peng, L.S. Turng, Electrospinning of unidirectionallu and orthogonally aligned thermoplastic polyurethane nanofibers: fiber orientation and cell migration. Soc. Biomater. **103**, 593–603 (2014)
71. G. Yang, M. Wang, J. Dong, F. Su, Y. Ji, C. Liu, C. Shen, Efficiency, fibers-induced segregated-like structure for polymer composites achieving excellent thermal conductivity and electromagnetic interference shielding. Compos. B **246**, 110253 (2022)
72. C.S. Kam, T.L. Leung, F. Liu, A.B. Djursic, M.H. Xie, W.-K. Chan, Y. Zhou, K. Shih, Lead removal from water-dependance on the form of carbon and surface functionalization. RSC Adv. **8**, 18355 (2018)
73. M.O. Shaikh, Y. Bin Huang, C.C. Wang, C.H. Chuang, Wearable woven triboelectric nanogenerator utilizing electrospun PVDF nanofibers for mechanical energy harvesting. Micromachines (2019). https://doi.org/10.3390/mi10070438